Determination of the intrinsic α/γ interface mobility during massive transformations in interstitial free Fe-X alloys

Zhu, Jianing; Luo, Haiwen; Yang, Zhigang; Zhang, Chi; van der Zwaag, Sybrand; Chen, Hao

DOI
10.1016/j.actamat.2017.05.045

Publication date
2017

Document Version
Accepted author manuscript

Published in
Acta Materialia

Citation (APA)
Zhu, J., Luo, H., Yang, Z., Zhang, C., van der Zwaag, S., & Chen, H. (2017). Determination of the intrinsic α/γ interface mobility during massive transformations in interstitial free Fe-X alloys. *Acta Materialia*, *133*, 258-268. https://doi.org/10.1016/j.actamat.2017.05.045

Postprint of Acta Materialia
Volume 133, July 2017, Pages 258–268
Link to formal publication (Elsevier): https://doi.org/10.1016/j.actamat.2017.05.045

Determination of the intrinsic α/γ interface mobility during massive transformations in interstitial free Fe-X alloys

Jianing Zhu[1], Haiwen Luo[2], Zhigang Yang[1], Chi Zhang[1],Sybrand van der Zwaag[3], Hao Chen[1]*

(1- Key Laboratory for Advanced Materials of Ministry of Education, School of Materials Science and Engineering, Tsinghua University, Beijing, China
(2- School of Metallurgical and Ecological Engineering, University of Science and Technology, Beijing, China
(3- Faculty of Aerospace Engineering, Delft University of Technology, Delft, the Netherlands)

Abstract

Kinetics of the austenite (γ) to ferrite (α) transformation and the reverse ferrite (α) to austenite (γ) transformation in a series of Fe-X (X=Ni, Mn and Co) binary alloys has been experimentally and theoretically investigated. A transition from partitioning to partitionless transformation has been predicted to occur during both the $\gamma \rightarrow \alpha$ and $\alpha \rightarrow \gamma$ transformations by a so called Gibbs Energy Balance (GEB) model, in which the chemical driving force is assumed to be equal to the energy dissipation due to interface friction and diffusion of X inside the migrating interfaces. The transition temperature is found to depend on the kind of X and its concentration, which is in good agreement with experimental results. The intrinsic mobility of the α/γ interface has been derived from the kinetic curves of both the $\gamma \rightarrow \alpha$ and $\alpha \rightarrow \gamma$

transformations in the investigated alloys, and its value seems to be marginally affected by the transformation direction and alloying elements.

Key Words: massive transformation; austenite; ferrite; interface mobility

* Email: hao.chen@mail.tsinghua.edu.cn; Tel: +86(0)62788328

1. Introduction

Over the past decades, the austenite (γ) to ferrite (α) transformation and the ferrite (α) to austenite (γ) transformation in the Fe-based alloys have received extensive concern due to their theoretical and practical importance [1-7]. In general, the diffusional phase transformations involve at least two process, the rearrangement of the crystal lattice and the redistribution of solute elements in the parent phase and new phase, and both of them could be the rate decisive process of the transformation, known as the diffusion-controlled transformation and the interface-controlled transformation, respectively [8]. However, the $\gamma \rightarrow \alpha$ and $\alpha \rightarrow \gamma$ transformations in the Fe-based alloys are usually situated between the pure diffusion-controlled and the pure interface-controlled transformation, e.g. a so called mixed-mode transformation, and deviation from the two extreme cases is strongly dependent on the value of the intrinsic α/γ interface mobility, which is a key physical parameter of phase transformations. Abundant effort has been made to determine the value of the intrinsic α/γ interface mobility during the $\gamma \rightarrow \alpha$ transformation due to its fundamental importance [9-13]. However, its exact value is still highly controversial, and the discrepancies among the values obtained by different research groups could be up to several orders of magnitude [14]. Furthermore, the value of the intrinsic α/γ

interface mobility during the $\alpha \rightarrow \gamma$ transformation has much less investigated. Theoretically speaking, the value of the intrinsic α/γ interface mobility should not depend on the transformation direction, e.g. the values of the intrinsic α/γ interface mobility during the $\gamma \rightarrow \alpha$ transformation and its reverse transformation should be the same, which needs to be further validated by experiments.

In order to derive the value of the α/γ interface mobility, much effort has been made to investigate the kinetics of the $\gamma \rightarrow \alpha$ transformation in the Fe-X (X is substitutional alloying element, e.g. Mn, Ni, et.al) alloys [15-18], during which a kinetic transition from the diffusion-controlled mode to the interface controlled mode (e.g. massive transformation) is expected to possibly occur [19-21]. In the diffusion-controlled mode, interface migration is expected to be extremely sluggish due to the very low diffusivity of the substitutional elements, while transformation kinetics should be significantly accelerated when the transformation shifts into the massive mode. Interface velocity during massive transformation is proportional to the available chemical driving force, and the proportionality is the intrinsic α/γ interface mobility. Kinetic transition during the $\gamma \rightarrow \alpha$ transformation in the Fe-Ni alloys has been investigated in reference [22-23], however, the effect of alloying elements and its concentration on the kinetic transition is still not well understood [24-26]. Compared with the $\gamma \rightarrow \alpha$ transformation, kinetic transition during the reverse $\alpha \rightarrow \gamma$ transformation upon heating has been relatively less discussed [27].

In this study, kinetics of the $\gamma \rightarrow \alpha$ and $\alpha \rightarrow \gamma$ transformations in a series of Fe-X (X=Ni, Mn, Co) alloys will be experimentally and theoretically investigated. A

so called Gibbs Energy Balance (GEB) model based on the solute drag theory, in which the energy dissipation due to interface friction and diffusion of alloying elements inside the migrating interface is assumed to be equal to the available chemical driving force, is utilized to predict kinetic transition during the $\gamma \rightarrow \alpha$ and $\alpha \rightarrow \gamma$ transformations. The value of the intrinsic mobility of the α/γ interface will be derived, and its dependence on transformation direction and alloying elements is discussed.

2. Experimental

A series of binary Fe-Ni, Fe-Mn and Fe-Co alloys are investigated in this study. Chemical composition of these alloys is shown in Table 1. Standard cylinder samples (4 mm in diameter and 10 mm in length) were machined for dilatometry experiments. A Bahr 805A dilatometer was used to measure the dilation of the specimens during the heat treatments. The samples were first heated to 950 ℃ for full austenization with a heating rate of 1 K/s, then held at 950 ℃ for 10 min and finally cooled down to room temperature with a cooling rate of 1 K/s. Kinetics of the austenite to ferrite transformation upon cooling and the ferrite to austenite transformation upon heating is derived from the dilatation curves using the level rule method. The heat treated samples were fine grinded and then etched using 2% Nital for optical microscopy observation.

The EBSD specimens were fine grinded and electrolytic polished with 20% $HClO_4$ and 80% C_2H_5OH for 20 s.

All thermodynamic data for the Fe-Ni, Fe-Mn and Fe-Co alloys used in this

study is calculated using ThermoCalc with TCFE6 database.

3. Model

A general mixed-mode model based on the principle of Gibbs Energy Balance (GEB) at the migrating interface is utilized to describe the kinetics of the austenite to ferrite and the ferrite to austenite transformations in the Fe-X binary alloys. The main assumption of the GEB approach is that at the migrating interfaces the available chemical driving force has to be balanced by the Gibbs energy dissipation due to diffusion of alloying elements inside the interface and interface friction during the transformation.

2.1 Chemical Driving Force

Chemical driving force at the migrating α/γ interfaces during the $\gamma \rightarrow \alpha$ transformation can be calculated as:

$$\Delta G_m^{chem} = \sum_i^n x_i^0 \left[\mu_i^{\gamma/\alpha}\left(x_i^{\gamma/\alpha}\right) - \mu_i^{\alpha/\gamma}\left(x_i^{\alpha/\gamma}\right) \right] \quad (1)$$

Where x_i^0 is the composition of the material transferred over the interface, *n* is the number of elements, $x_i^{\gamma/\alpha}$ and $x_i^{\alpha/\gamma}$ are the mole fractions of the element *i* at the interface on the austenite and ferrite side, respectively. $\mu_i^{\gamma/\alpha}$ and $\mu_i^{\alpha/\gamma}$ are the chemical potential of *i* in austenite and ferrite. For the binary Fe-X alloys, the chemical driving force for the $\gamma \rightarrow \alpha$ transformation can be simplified as:

$$\Delta G_m^{chem} = G_m^{\gamma} - G_m^{\alpha} \quad (2)$$

Where G_m^{γ} and G_m^{α} are the mole Gibbs energy of ferrite and austenite with the nominal composition, respectively. The chemical driving force at the migrating α/γ interface during the $\alpha \rightarrow \gamma$ transformation can be calculated in the same way.

2.2 Dissipation of Gibbs energy

The dissipation of Gibbs energy can be divided into two parts: (i) Dissipation due to diffusion inside the interface and (ii) Dissipation due to the movement of atoms responsible for the change of crystalline structure, which is also called as the interface friction.

During the $\gamma \rightarrow \alpha$ and $\alpha \rightarrow \gamma$ transformations, substitutional alloying elements tend to segregate into the migrating interfaces. The degree of segregation depends on binding energy of the substitutional alloying element, chemical potential difference of the substitutional alloying elements in γ and α phase, and interface velocity. In this work, a triangular potential well, as proposed by Purdy and Bréchet [28], is assumed inside the interface. μ_0^{α} and μ_0^{γ} are the chemical potential of the substitutional alloying elements in ferrite and austenite, respectively; E_0 is the binding energy; ΔE is half of chemical potential difference of substitutional alloying elements in austenite and ferrite, and its value depends on temperature and the partition coefficient of the substitutional element; δ is the half thickness of the interface.

The governing equation for alloying elements diffusion inside the interface migrating with a quasi-steady velocity v is [28]:

$$\frac{\partial}{\partial x}\left[D\frac{\partial X}{\partial x}+\frac{DX}{RT}\frac{\partial E}{\partial x}+vX \right]=0 \tag{3}$$

where X is the concentration of substitutional alloying elements, x is distance, D is the diffusion coefficient of substitutional alloying elements inside the α/γ interface, R is gas constant, T is temperature, v is the interface velocity, and E is the free energy of

interaction of the substitutional alloying elements with the interface.

The solution of equation (3) is as follows:

$$\frac{X}{X_0}=1\,,\quad \text{for } S<-1 \tag{4}$$

$$\frac{X}{X_0}=\frac{1+ae^{\left(-V(1+a)(1+S)\right)}}{1+a}\,,\quad \text{for } -1<S<0 \tag{5}$$

$$\frac{X}{X_0}=\frac{1+\left(\dfrac{a(1+b)e^{\left(-V(1+a)\right)}}{1+a}+\dfrac{b-a}{1+a}\right)e^{-V(1+b)S}}{1+b}\,,\quad \text{for } 0<S<1 \tag{6}$$

$$\frac{X}{X_0}=1+e^{-VS}\left(\frac{ae^{\left(-V(1+a+b)\right)}}{1+a}+\frac{(b-a)e^{(-Vb)}}{(1+a)(1+b)}-\frac{be^{V}}{1+b}\right),\quad \text{for } 1<S \tag{7}$$

where X_0 is the nominal concentration of the substitutional alloying elements in the alloys and S, v, a, b are all dimensionless quantities defined as:

$$a=\frac{D(\Delta E-E_0)}{RTv\delta}\,,\quad \mathrm{b}=\frac{D(\Delta E+E_0)}{RTv\delta}\,,\quad V=\frac{v\delta}{D}\,,\quad S=\frac{X}{\delta}$$

Dissipation due to diffusion of substitutional alloying elements inside the α/γ interface can be calculated using Cahn's equation [29]:

$$\Delta G_{diff}=-\int_{-\delta}^{\delta}(X-X_0)\left(\frac{dE}{dx}\right)dx \tag{8}$$

Particularly, at ultra-low interface velocity $v\rightarrow 0$, the interfacial dissipation is given by:

$$\Delta G_{diff}=2X_0\Delta E+RTX_0(e^{\frac{-2\Delta E}{RT}}-1) \tag{9}$$

which is not dependent on the interface thickness, diffusion coefficients of substitutional alloying elements and binding energy.

The energy dissipation due to interface friction is given by:

$$\Delta G_{fri}=v/M_{int} \tag{10}$$

where v is interface velocity and M_{int} is the intrinsic interface mobility.

2.3 Gibbs Energy Balance at the interface

According to the GEB concept, the chemical driving force has to be equal to the energy dissipation during the transformation.

$$\Delta G_m^{chem} = \Delta G_{diff} + \Delta G_{fri} \tag{11}$$

It should be mentioned that for all the mathematical expressions in the model, no restriction on the transformation direction is presumed. In other words, this model can be applied to both the $\alpha \rightarrow \gamma$ and the $\gamma \rightarrow \alpha$ transformation.

4. Results and Discussion

4.1 Experimental results

4.1.1 Microstructures

Microstructures of the specimens were observed by optical microscope and EBSD. Figure 1a and 1b show the EBSD maps of the Fe-3Mn alloy before and after the heat treatment respectively. For all the investigated samples, the microstructure was massive ferrite and it was found that after one cycle of heat treatment, both the morphology and average grain size of the sample did not change much.

4.1.2 Kinetics of the austenite to ferrite transformation

In Fig. 2, the overall kinetics of the $\gamma \rightarrow \alpha$ transformation upon cooling at a rate of 1 K/s in a series of Fe-Ni, Fe-Mn and Fe-Co alloys is shown (data for Fe-1Mn and Fe-2Mn alloys is obtained from [9], and the cooling rate is 20 K/min, however, cooling rate does not significantly affect the onset temperature of the transformation). The $\gamma \rightarrow \alpha$ transformation is very fast, and it is finished in about one minute. Ni

and Mn concentration significantly affects the starting temperature of the $\gamma \rightarrow \alpha$ transformation (F_s), which is found to decrease with increasing Ni and Mn concentration and be lower than both A_{e3} and T_0 . However, it is interesting that the effect of Co concentration on the F_s is negligible. In Fig. 3, deviation of F_s from T_0 for the Fe-Ni, Fe-Mn and Fe-Co alloys is plotted as a function of solute concentration, which will be discussed in the following sections.

The interface velocity during the $\gamma \rightarrow \alpha$ transformation can be estimated from the transformation curves using the following equation [30]:

$$.df / dt = 3(N^* g)^{(1/3)}(1-f^2)v_{\alpha/\gamma} arctanh^{(2/3)}(f) \quad (12)$$

where f is the fraction of ferrite; N^* is the density of nuclei per volume, it can be estimated as d^{-3}, and d is the average grain size of the ferrite; g is the geometrical factor (g=1 for cubic growth and g= 4π /3 for spherical growth), $v_{\alpha/\gamma}$ is the velocity of the α/γ interface. In Fig. 4a, the derived interface velocity as a function of ferrite fraction in the Fe-1.5Ni alloys is indicated. It is found that interface velocity is almost constant during the entire transformation, which is regarded as a typical feature of massive transformation. In Fig. 4b, the derived average interface velocities during the $\gamma \rightarrow \alpha$ transformation in the Fe-Ni, Fe-Mn and Fe-Co alloys as a function of solute concentration are shown. In general, the average interface velocity decreases slightly with increasing solute concentration. Some of this reduction may also be due to the fact that for higher concentrations the transformation takes place at lower temperatures as shown in figure 2.

4.1.3 Kinetics of the ferrite to austenite transformation

In Fig. 5, overall kinetics of the ferrite to austenite transformation upon heating at a rate of 1 K/s in a series of Fe-Ni, Fe-Mn and Fe-Co alloys is shown. Similar as the $\gamma \rightarrow \alpha$ transformation, Ni and Mn have a significant effect on the starting temperature for the $\alpha \rightarrow \gamma$ transformation (*As*), which is experimentally found to increase with decreasing Mn or Ni concentration and is much higher than T_0 and A_{e1}. Co has a negligible effect on the A_s. Deviations of A_s from T_0 for the Fe-Ni, Fe-Mn and Fe-Co alloys are plotted as a function of Ni, Mn and Co concentration in Fig. 3 as well.

The interface velocities during the $\alpha \rightarrow \gamma$ transformation in the Fe-Ni, Fe-Mn and Fe-Co alloys are also calculated using equation (12). The average grain size of austenite was estimated as 50 μm in the calculation. Fig. 6a. shows the interface velocity as a function of austenite fraction in the Fe-1.5Ni and Fig. 6b shows the average interface velocities in all the investigated alloys. It is found that the interface velocities during the $\alpha \rightarrow \gamma$ transformation are in the same order as those during the $\gamma \rightarrow \alpha$ transformation and also decrease with increasing solute concentration.

4.2 Theoretical analysis

In principle, the austenite to ferrite transformation in the substitutional binary alloys could proceed in either partitioning or partitionless mode. Thermodynamically speaking, the partitioning transformation upon cooling is expected to start once temperature is lower than A_{e3}, while the partitionless transformation should start below T_0. However, the experimental results indicate that the starting temperatures for the partitionless austenite to ferrite transformation (e.g. massive transformation) in the

Fe-Ni and Fe-Mn alloys are significantly lower than T_0, and the magnitude of deviation is Ni and Mn concentration dependent.

In this section, the GEB model is applied to simulating the kinetic transition from partitioning to partitionless mode during the austenite to ferrite transformation and the ferrite to austenite in the binary alloys. In the simulations, the α/γ interface thickness 2δ is assumed to be 0.5 nm. Diffusion coefficients of the substitutional elements inside the α/γ interface are assumed to be the geometric average of diffusion coefficients in austenite and in ferrite [31-33], which are calculated from DICTRA. The values of chemical potential of the substitutional elements in α and γ are calculated by ThermoCalc with TCFE6 database. The binding energies of Ni, Mn and Co are chosen to be 5 kJ/mol, 9.9 kJ/mol and 3 kJ/mol, respectively [34-35]. The interface mobility is assumed to be 0.058exp(-140000/RT) mmol/J·s suggested by Krielaart [9].

In Fig. 7, the energy dissipations due to Ni diffusion inside the migrating interface and interface friction as a function of interface velocity for the γ→α transformation in the Fe-3Ni alloy at 715 ℃ are shown. The energy dissipation due to Ni diffusion inside the interface is almost constant when interface velocity is lower than 10^{-9} m/s. It starts to decrease rapidly when interface velocity is higher than 10^{-9} m/s and finally approaches almost zero when interface velocity is about 10^{-6} m/s. Dissipation due to interface friction is proportional to interface velocity, and the proportionality is the interface mobility. The dissipation due to the interfacial diffusion and interface friction are the dominant constituents of the total energy

dissipation at the low interface velocity zone and the high interface velocity zone, respectively. However, the chemical driving force at the migrating α/γ interface is constant at a given temperature.

In Fig. 8a and 8b, the total energy dissipation and chemical driving force as a function of interface velocity for the γ→α transformation in the Fe-3Ni alloy at 730 ℃ and 715 ℃are indicated. According to the GEB concept, at the migrating interface the available chemical driving force has to be balanced by the total energy dissipation. In other words, the intersection between the chemical driving force curve and the total dissipation curve yields the interface velocity at that moment of the transformation.

At 730 ℃, although there is large chemical driving force available for the γ→α transformation, it is not large enough to exceed the dissipation barrier. Therefore, it is predicted that at 730 ℃ the γ/α interface has to migrate in a mode that involves the long range diffusion of Ni. The kinetics of interface migration is controlled by Ni diffusion and is extremely sluggish. By solving Ni diffusion and mass balance equations, interface velocity can be estimated as [36]:

$$v = \frac{D_{Ni}^{\gamma}(C_{Ni}^{\gamma} - C_{\mathrm{Ni}}^{0})^{2}}{2(C_{Ni}^{\gamma} - C_{Ni}^{\alpha})(C_{Ni}^{0} - C_{Ni}^{\alpha})\lambda} \tag{13}$$

where D_{Ni}^{γ} is the diffusion coefficient of Ni in austenite, λ is the half thickness of ferrite , C_{Ni}^{0} is the nominal Ni concentration, C_{Ni}^{γ} and C_{Ni}^{α} are the equilibrium Ni concentration in austenite and ferrite, respectively. Assuming λ is 100 nm, interface velocity is estimated to be in the order of 10^{-11}~10^{-12} m/s, which is too sluggish to be detected in the current dilatometry experiments.

At 715 ℃, chemical driving force at the migrating interface is large enough to

overcome the dissipation barrier, and it intersects with the total energy dissipation curve at a very high interface velocity (around 10^{-7} m/s). There is no diffusion of Ni inside the interface, and chemical driving force is fully dissipated by the interface friction. In other words, the $\gamma \rightarrow \alpha$ transformation at 715 ℃ is partitionless. The value of the γ/α interface mobility is still very controversial, and there is a large discrepancy among those measured by different research groups. Two other values of M are assumed in the calculations of Figure 8b, e.g. (i) $M=5\times10^{3}\exp(-147000/RT)$ mmol/J·s suggested by Hillert; and (ii) $M=2.4\exp(-140000/RT)$ mmol/J·s suggested by Wits. The predicted interface velocity at 715 ℃ is strongly dependent on the assumed value of interface velocity, and it is ranged from 10^{-7} to 10^{-3} m/s depending on the selection of M. The predicted features of the austenite to ferrite transformation at 715℃ is fit with the definition of massive transformation.

In Fig. 9a, the predicted interface velocities as a function of temperature are shown for the Fe-Ni alloys with different Ni concentration, and the corresponding T_0 temperatures are labelled with the solid arrows. In the simulations, the value of interface mobility is assumed to be $M=0.058\exp(-140000/RT)$ mmol/J·s. Kinetic transition from partitioning to partitionless upon cooling is predicted to occur at a critical temperature (T_c), which is lower than T_0 and depends on Ni concentration. It is well known that T_0 is regarded as the thermodynamic limit for partitionless transformation. In other words, extra chemical driving force is required to activate the partitionless austenite to ferrite transformation in the Fe-Ni alloys. The magnitude of the extra chemical driving force required to initiate the partitionless transformation

increases with increasing Ni concentration, which is because the energy dissipation caused by Ni diffusion inside the interface is proportional to Ni concentration. Similar calculations have also been made for the austenite to ferrite transformation in the Fe-Mn and Fe-Co alloys, as shown in Fig. 9b and 9c. Increment of Mn concentration significantly reduces T_c while Co concentration has almost no effect on T_c.

The kinetics of austenite reversion in the Fe-Ni alloys can be calculated based on the GEB model as well. Fig. 10 show the total energy dissipation together with the available chemical driving force at the migrating interface at 800 ℃ and 810 ℃ for the $\alpha \rightarrow \gamma$ transformation in the Fe-3Ni alloy, respectively. At 800 ℃, although there is available chemical driving force for the $\alpha \rightarrow \gamma$ transformation, it is not large enough to overcome the dissipation barrier. Thus the transformation has to proceed in the mode that involves the long range diffusion of Ni in austenite and ferrite. The interface velocity is controlled by Ni diffusion, and the transformation kinetics is expected to be too sluggish to be detected in the current experiments. However, at 810 ℃, the chemical driving force is large enough to overcome the dissipation barrier. The $\alpha \rightarrow \gamma$ transformation is able to proceed in a partitionless mode, and the interface velocity is determined by interface mobility. In Fig. 11a, the predicted interface velocities during the ferrite to austenite transformation in the Fe-Ni alloys are shown as a function of temperature. Similar as the $\gamma \rightarrow \alpha$ transformation, a kinetic transition is predicted to occur at a critical temperature (T_c), which is higher than T_0 and is Ni concentration dependent.

The predicted interface velocities as a function of temperature during the ferrite

to austenite transformation for the Fe-Mn and Fe-Co alloys are calculated as well and are shown in Fig. 11b and 11c. It is predicted that Co has a very marginal effect on T_c, which is in good agreement with experimental results.

4.3 Discussion

4.3.1 Kinetic transition

As mentioned in section 4.2, kinetic transition from partitioning to partitionless transformation during the austenite to ferrite transformation and the ferrite to austenite transformation has been predicted by the GEB approach, and the critical temperature (T_c) at which the transition occurs is regarded as the starting temperature for the massive transformation. In Fig. 12a-12c, a comparison between the predicted and measured onset temperatures for the austenite to ferrite and ferrite to austenite transformation in the Fe-Ni, Fe-Mn and Fe-Co alloys are plotted in their phase diagrams. It shows that the GEB predictions are in good agreement with the experimental results, while the experimentally determined transformation starting temperatures deviate from T_0.

Nucleation incubation could also be argued to be a possible reason for the deviation between experiments and T_0. In order to rule out nucleation effect, a specific experiment has been designed to study ferrite or austenite formation from a mixture of austenite and ferrite, and its temperature program is shown in Fig. 13a. In the first temperature cycle, the $\alpha \rightarrow \gamma$ transformation upon heating was interrupted at 795 ℃ to obtain a mixture of ferrite and austenite, which was then cooled down to 450 ℃ (AB) for the $\gamma \rightarrow \alpha$ transformation. The measured dilation is indicated in Fig. 13b.

It shows that the starting temperature of the partitionless $\gamma \rightarrow \alpha$ transformation from a mixture of austenite and ferrite is almost the same as that of the partitionless $\gamma \rightarrow \alpha$ transformation from full austenite, which means that the deviation between the experimentally determined starting temperature and T_0 should not be caused by nucleation incubation. In the second temperature cycle, the $\gamma \rightarrow \alpha$ transformation upon cooling was interrupted at 600 ℃ to obtain a mixture of austenite and ferrite, and the sample is then heated to 900 ℃ (CD) for the $\alpha \rightarrow \gamma$ transformation. Similarly, the starting temperature for the $\alpha \rightarrow \gamma$ transformation is not affected by reserved austenite.

Both experiments and model predictions have indicated that the effects of Ni, Mn and Co on the kinetic transition are different. Based on thermodynamic calculations, it has been found that the $\triangle E$ for Mn and Ni is much larger than Co. Therefore, it is expected that the energy dissipation by the interfacial diffusion of Mn or Ni should be much larger than Co, which well explains why the starting temperatures for the partitionless transformation in the Fe-Ni and Fe-Mn alloys deviate significantly from T_0 for the $\gamma \rightarrow \alpha$ or $\alpha \rightarrow \gamma$ transformation while in the Fe-Co alloys the starting temperature for partitionless transformation is close to T_0.

4.3.2 The α/γ interface mobility

Two kinds of interface mobility have been discussed in literature: the effective interface mobility M_{eff} and the intrinsic interface mobility M_{int} [37-38]. The intrinsic interface mobility corresponds to the Gibbs energy dissipated by lattice rearrangement only, hence reflects the intrinsic feature of the migrating interface itself.

It is believed that the intrinsic mobility has an Arrhenius relationship with temperature:

$$M_{int} = M_0 exp\left(-\frac{Q}{RT}\right) = v/\Delta G_{fri} \quad (14)$$

where M_0 is a pre-exponential constant, Q is the activation energy, R is the gas constant , T is the temperature and ΔG_{fri} is the Gibbs energy dissipated by lattice rearrangement. On the other hand, the effective interface mobility includes the effects of various dissipative process such as lattice rearrangement, solute drag effect, etc. As a result, its value could change with alloying elements concentration, transformation directions or some other factors.

The value of the effective or intrinsic interface mobility is usually obtained by fitting transformation curves with kinetic models in the literature. In the current study, both the austenite to ferrite transformation and the ferrite to austenite transformation occur in a partitionless mode, which means that the energy dissipation is fully owing to lattice arrangement. The intrinsic α/γ interface mobility is derived by fitting the current experiments with the GEB model, as shown in Fig. 14. Because the transformation starting temperatures for the ferrite to austenite transformation in the Fe-0.5Co and Fe-1.5Co alloys are slightly lower than T_0, the derived mobility for these two alloys during the $\alpha \rightarrow \gamma$ transformation is not shown. It can be concluded from the diagram that (1) the logarithm of the intrinsic α/γ interface mobility has an approximate linear function with 10000/T. Therefore, the intrinsic α/γ interface mobility follows the Arrhenius relationship assumption. (2) The α/γ interface mobility in the investigated Fe-Ni, Fe-Mn and Fe-Co alloys can be estimated as $M = 2.7 \times$

$10^{-6}\exp(-145000/RT)$ $m^4/J\cdot s$. (3) The value of the intrinsic α/γ interface mobility is found to be marginally dependent on migration direction of the interface, the kind of substitutional alloying element and its concentration, which is in accordance with the "intrinsic" definition of the intrinsic mobility.

Conclusion

Kinetics of the austenite to ferrite transformation upon cooling and the ferrite to austenite transformation upon heating in a series of Fe-Ni, Fe-Mn and Fe-Co alloys have been investigated in order to shed new light on the mechanism of kinetic transition from partitioning to partitionless transformation and the intrinsic α/γ interface mobility. The following conclusions can be drawn:

1) The transition from partitioning to partitionless transformation could occur during both the $\gamma \rightarrow \alpha$ and $\alpha \rightarrow \gamma$ transformations, and the transition temperature is found to deviate from T_0 to some degree depending on the nature of alloying element and its concentration. The GEB model can well describe the kinetic transition for both the $\alpha \rightarrow \gamma$ and $\gamma \rightarrow \alpha$ transformation.

2) Intrinsic mobility of the α/γ interface is derived based on the transformation curves of a series of Fe-Ni, Fe-Mn and Fe-Co alloys, and it is found that the value of intrinsic interface mobility depends marginally on the transformation direction, the kind of alloying element and its concentration. The intrinsic interface mobility can be written as $2.7 \times 10^{-6}\exp(-145000/RT)$ $m^4/J\cdot s$.

ACKNOWLEDGEMENTS

The support from the National Natural Science Foundation of China (Grant 51501099 and 51471094) is acknowledged. Haiwen Luo is grateful to the joint financial support from National Natural Science Foundation of China and Bao Steel Group Co. Ltd (Grant U1460203). H. Chen acknowledges financial support from National Young 1000-Talents Program (D1101073).

Reference

[1] S. E. Offerman, N. H. van Dijk, J. Sietsma, S. Grigull, E. M. Lauridsen, L. Margulies, H. F. Poulsen, M. Th. Rekveldt, S. van der Zwaag, Grain Nucleation and Growth During Phase Transformations, Science 298 (2002) 1003–1005

[2] C.R. Hutchinson, A. Fuchsmann, H.S. Zurob, Y. Brechet, A novel experimental approach to identifying kinetic transitions in solid state phase transformations, Scripta Mater. 50 (2004) 285–289.

[3] H. Chen, Y.C. Liu, Z. Sheng, Y.L. Li, L.F. Zhang, Consideration of the growth mode in isochronal austenite-ferrite transformation of ultra-low-carbon Fe–C alloy, Appl. Phys. A 98 (2010) 211–217.

[4] Hao Chen, Benoît Appolaire, Sybrand van der Zwaag, Application of cyclic partial phase transformations for identifying kinetic transitions during solid-state phase transformations: Experiments and modeling, Acta Mater. 59 (2011) 6751–6760.

[5] Z.-Q. Liu, G. Miyamoto, Z.-G. Yang, T. Furuhara, Direct measurement of carbon enrichment during austenite to ferrite transformation in hypoeutectoid Fe–2Mn–C

alloys, Acta Mater. 61 (2013) 3120–3129.

[6] R. Wei, M. Enomoto, R. Hadian, H.S. Zurob, G.R. Purdy, Growth of austenite from as-quenched martensite during intercritical annealing in an Fe–0.1C–3Mn–1.5Si alloy, Acta Mater. 61 (2013) 697–707.

[7] C. Qiu, H.S. Zurob, C.R. Hutchinson, The coupled solute drag effect during ferrite growth in Fe–C–Mn–Si alloys using controlled decarburization, Acta Mater. 100 (2015) 333–343.

[8] Jilt Sietsma, Sybrand van der Zwaag, A concise model for mixed-mode phase transformations in the solid state, Acta Mater. 52 (2004) 4143–4152.

[9] G. P. Krielaart, S. van der Zwaag, Kinetics of $\gamma \rightarrow \alpha$ phase transformation in Fe-Mn alloys containing low manganese, Mater. Sci. Tech. 14 (1998) 10–18.

[10] J.J. Wits, T.A. Kop, Y. van Leeuwen, J. Seitsma, S. van Der Zwaag, A study on the austenite-to-ferrite phase transformation in binary substitutional iron alloys, Acta Mater. 54 (2000) 1431–1440.

[11] C. Bos,, F. Sommer, E.J. Mittemeijer, An atomistic analysis of the interface mobility in a massive transformation, Acta Mater. 53 (2005) 5333–5341.

[12] Gamsjäger, M. Militzer, F. Fazeli, J. Svoboda, F.D. Fischer, Interface mobility in case of the austenite-to-ferrite phase transformation, Comp. Mater. Sci. 37 (2006) 94–100.

[13] M.G. Mecozzi, J. Sietsma, S. van der Zwaag, Analysis of $\gamma \rightarrow \alpha$ transformation in a Nb micro-alloyed C-Mn steel by phase field modelling, Acta Mater. 54 (2006) 1431–1440.

[14] M. Hillert, L. Höglund, Mobility of a/c phase interfaces in Fe alloys, Scripta Mater. 54 (2006) 1259–1263.

[15] T.B. Massalski, J.H. Perepezko, J. Jaklovsky, A microstructural study of massive transformations in the Fe--Ni system Mater. Sci. Eng. 18 (1975) 193–198.

[16] Y. C. Liu, F. Sommer, E. J. Mittemeijer, Abnormal austenite–ferrite transformation behaviour in substitutional Fe-based alloys, Acta Mater. 51 (2003) 507–519.

[17] Y. C. Liu, F. Sommer, E. J. Mittemeijer, Kinetics of the abnormal austenite–ferrite transformation behaviour in substitutional Fe-based alloys. Acta Mater. 52 (2004) 2549-2560.

[18] J. Hamada, M. Enomoto, T. Fujishiro, In-Situ observation of the growth of massive ferrite in very low-carbon Fe-Mn and Ni Alloys, Metall. Mater. Trans. A 45 (2014) 3781–3789.

[19] J. Ågren, A simplified treatment of the transition from diffusion controlled to diffusion-less growth, Acta Metall. 37 (1989) 181–189.

[20] I. Loginova, J. Odqvist , G. Amberg, J. Ågren. The phase-field approach and solute drag modeling of the transition to massive $\gamma \rightarrow \alpha$ transformation in binary Fe-C alloys, Acta Mater. 51 (2003) 1327–1339.

[21] Y.C. Liu, F. Sommer, E.J. Mittemeijer, The austenite–ferrite transformation of ultralow-carbon Fe–C alloy; transition from diffusion- to interface-controlled growth, Acta Mater. 54 (2006) 3383–3393.

[22] A. Borgenstam, M. Hillert, Massive transformation in the Fe-Ni system, Acta

Mater. 48 (2000) 2765–2775.

[23] J. Odqvist, On the transition to massive growth during the γ → α transformation in Fe‐Ni alloys, Scripta Mater. 52 (2005) 193‐197.

[24] M. Hillert, Thermodynamics of the massive transformation, Metall. Mater. Trans. A 15A (1984) 411–419.

[25] Y.J.M. Bréchet, G.R. Purdy, On solute drag in the massive transformation, Scripta Mater. 27 (1992) 1753–1757.

[26] M. Hillert, M. Schalin, Modeling of solute drag in the massive phase transformation, Acta Mater. 48 (2000) 461–468.

[27] Ji-Hye Park, Young-Kook Lee, Non-isothermal austenite formation behavior in an interstitial free steel with different ferrite microstructures, Scripta Mater. 58 (2008) 602–605.

[28] G.R. Purdy, Y.J.M. Bréchet, A solute drag treatment of the effects of alloying elements on the rate of the proeutectoid ferrite transformation in steels, Acta Metall. Mater. 43(1995) 3763–3774.

[29] J.W. Cahn, The impurity-drag effect in grain boundary motion, Acta Metall. 10 (1962) 789–798.

[30] A.T.W. Kempen, F. Sommer, E.J. Mittemeijer, The kinetics of the austenite–ferrite phase transformation of Fe-Mn: differential thermal analysis during cooling, Acta Mater. 50 (2002) 3545–3555.

[31] A. Béché, H.S. Zurob, C.R. Hutchinson, Quantifying the solute drag effect of Cr on ferrite growth using controlled decarburization experiments, Metall. Mater. Trans.

A 38A (2007) 2950–2955.

[32] C. Qiu, H.S. Zurob, D. Panahi, Y.J.M. Bréchet, G.R. Purdy, C.R. Hutchinson, Quantifying the solute drag effect on ferrite growth in Fe-C-X alloys using controlled decarburization experiments, Metall. Mater. Trans. A 44A (2013) 3472–3483.

[33] T. Jia, M. Militzer, The effect of solute Nb on the austenite-to-ferrite transformation, Metall. Mater. Trans. A 46A (2015) 614–621.

[34] M. Enomoto, C.L. White, H.I. Aaronson, Evaluation of the effects of segregation on austenite grain boundary energy in Fe-C-X alloys, Metall. Mater. Trans. A 19A (1988) 1807–1818.

[35] H. Chen, S. van der Zwaag, A general mixed-mode model for the austenite-to-ferrite transformation kinetics in Fe–C–M alloys, Acta Mater. 72 (2014) 1–12.

[36] C. Zener, Theory of growth of spherical precipitates from solid solution, J. Appl. Phys. 20 (1949) 950–953.

[37] Ernst Gamsjäger, Hao Chen, Sybrand van der Zwaag, Application of the cyclic phase transformation concept for determining the effective austenite/ferrite interface mobility, Comp. Mater. Sci. 83 (2014) 92–100

[38] E. Gamsjäger, M. Wiessner, S. Schider, H. Chen, S. van der Zwaag, Analysis of the mobility of migrating austenite–ferrite interfaces, Philos. Mag. 95 (2015) 2899–2917.

Figure Captions

Figure 1. EBSD maps of the Fe-3Mn alloy (a) before and (b) after the heat treatment

Figure 2. Overall kinetics of the austenite to ferrite transformation upon cooling at a rate of 1 K/s in the Fe-Ni, Fe-Mn and Fe-Co alloys.

Figure 3. Deviations of F_s and A_s from T_0 upon cooling and heating in the Fe-Ni, Fe-Mn and Fe-Co alloys as a function of the solute concentration.

Figure 4. (a) The interface velocity as a function of ferrite fraction in the Fe-1.5Ni alloy. (b) The average interface velocities during the austenite to ferrite transformation as a function of solute concentration.

Figure 5. Overall kinetics of the ferrite to austenite transformation upon heating at a rate of 1 K/s in the Fe-Ni, Fe-Mn and Fe-Co alloys.

Figure 6. (a) The interface velocity as a function of austenite fraction in the Fe-1.5Ni alloy. (b) The average interface velocities during the ferrite to austenite transformation as a function of solute concentration.

Figure 7. The energy dissipation at the migrating interface as a function of interface velocity during the austenite to ferrite transformation in the Fe-3Ni alloy at 715 ℃.

Figure 8. Total Gibbs energy dissipation and the available chemical driving force as a function of interface velocity for the $\gamma \rightarrow \alpha$ transformation in an Fe-3Ni alloy (a) at 730 ℃and (b) at 715 ℃.

Figure 9. The predicted interface velocities as a function of temperature for the $\gamma \rightarrow \alpha$ transformation in (a) Fe-Ni (b) Fe-Mn and (c) Fe-Co alloys. The corresponding T_0 temperatures are labelled with the solid arrows.

Figure 10. Total Gibbs energy dissipation and the available chemical driving force as a function of interface velocity for the α → γ transformation in Fe-3Ni (a) at 800 ℃ and (b) at 810 ℃.

Figure 11. The predicted interface velocities as a function of temperature for the α → γ transformation in (a) Fe-Ni (b) Fe-Mn and (c) Fe-Co alloys with different solute concentration. The corresponding T_0 temperatures are labelled with the solid arrows.

Figure 12. Comparison between model predictions and experimental measurements of the onset temperatures for the austenite to ferrite transformation and ferrite to austenite transformations in the (a) Fe-Ni (b) Fe-Mn and (c) Fe-Co alloys.

Note: (1) Experimental data of the Fe-1Mn and Fe-2Mn alloys are obtained from [9].

(2) The A_{e1}, A_{e3} and T_0 lines overlap in the Fe-Co diagram so that only one solid line is visible.

Figure 13. (a) Sketch of heat treatment (b) Dilatation curve of the specimen as a function of temperature.

Figure 14. The derived intrinsic interface mobility as a function of temperature.

Table 1. Chemical composition of the investigated alloys (all in wt.%).

Alloy	Solute concentration,wt.%	A_{e1}, ℃	T_0, ℃	A_{e3}, ℃
Fe-0.5Ni	0.54.	874	884	890
Fe-1Ni	1.07	838	859	871
Fe-1.5Ni	1.26.	805	835	853
Fe-3Ni	3.13	706	775	809
Fe-1Mn	0.88[9]	834	855	868
Fe-2Mn	1.98[9]	754	806	831
Fe-3Mn	2.78	630	761	798
Fe-0.5Co	0.52	912	912	912
Fe-1.5Co	1.50	913	913	913

Note: Data for the Fe-1Mn and Fe-2Mn alloys is obtained from [9].

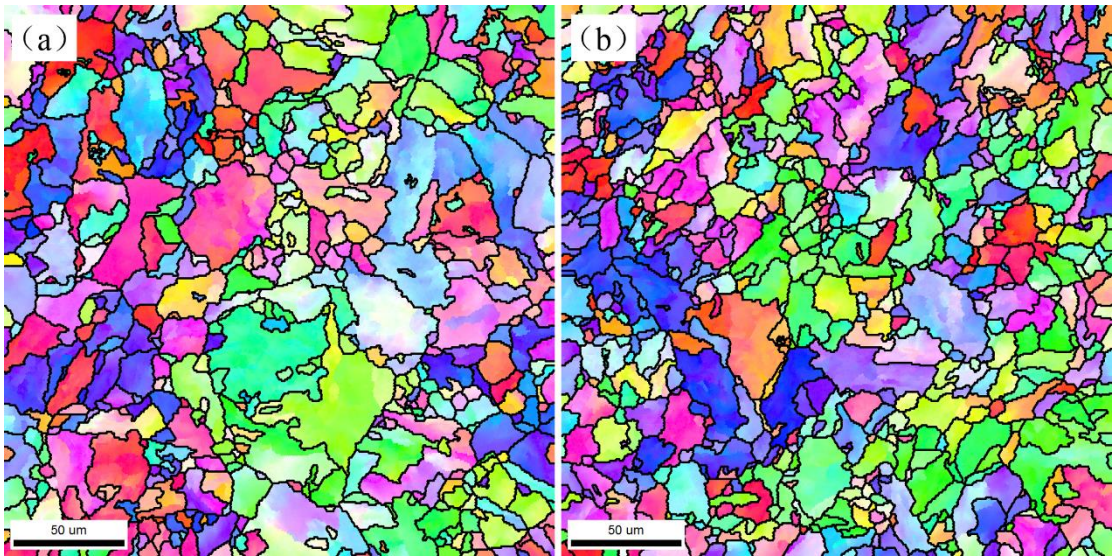

Fig. 1 EBSD maps of the Fe-3Mn alloy (a) before and (b) after the heat treatment

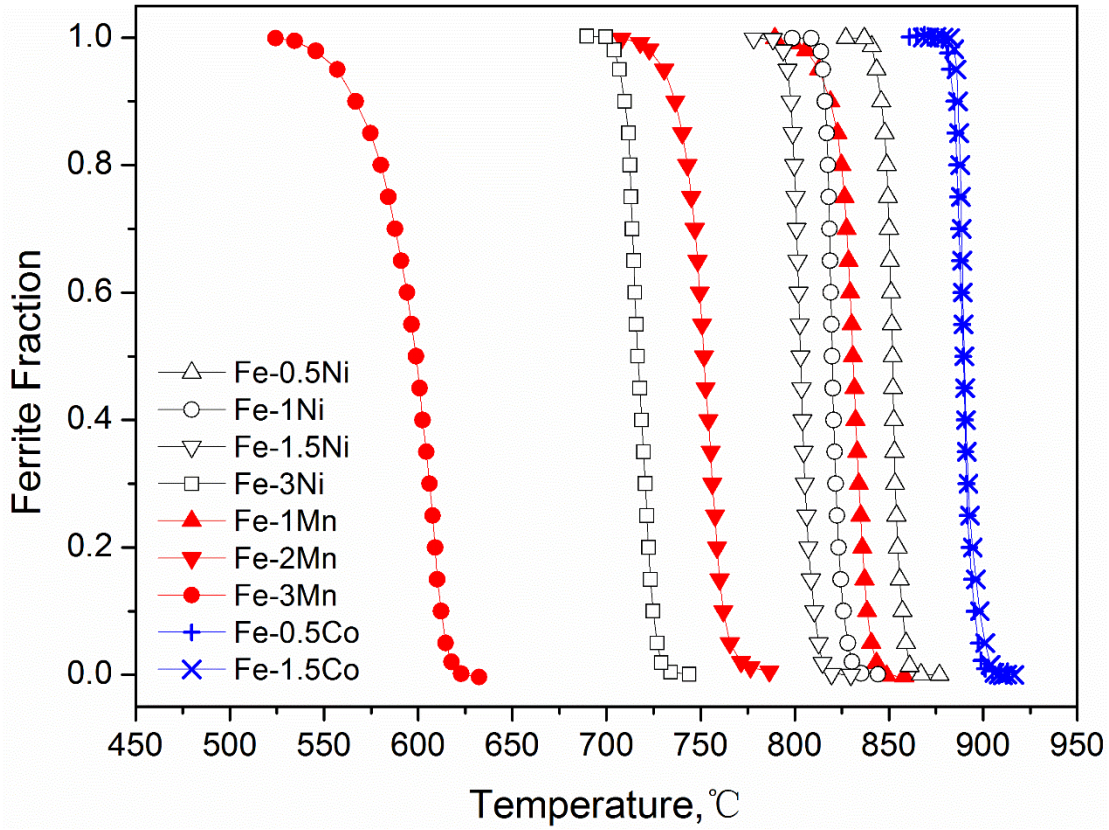

Fig. 2 Overall kinetics of the austenite to ferrite transformation upon cooling at a rate of 1 K/s in the Fe-Ni, Fe-Mn and Fe-Co alloys.

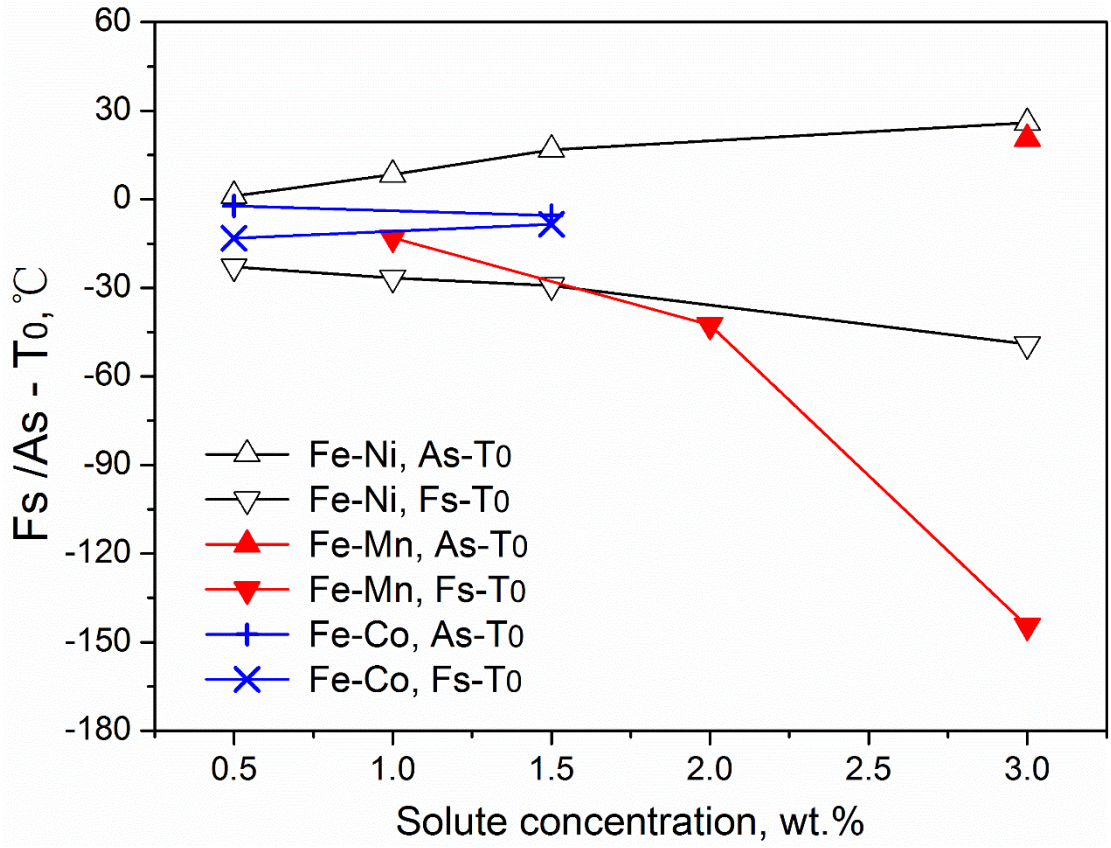

Fig. 3 Deviations of F_s and A_s from T_0 upon cooling and heating in the Fe-Ni, Fe-Mn and Fe-Co alloys as a function of the solute concentration.

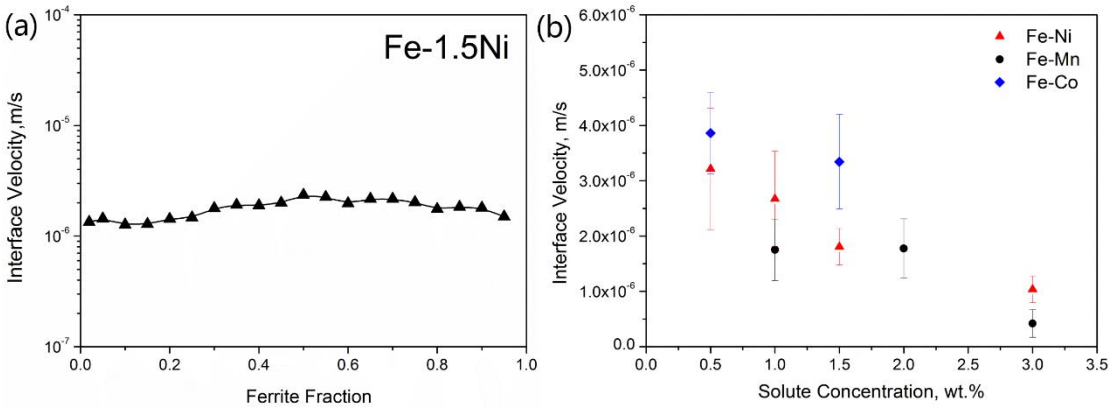

Fig. 4 (a) The interface velocity as a function of ferrite fraction in the Fe-1.5Ni alloy. (b) The average interface velocities during the austenite to ferrite transformation as a function of solute concentration.

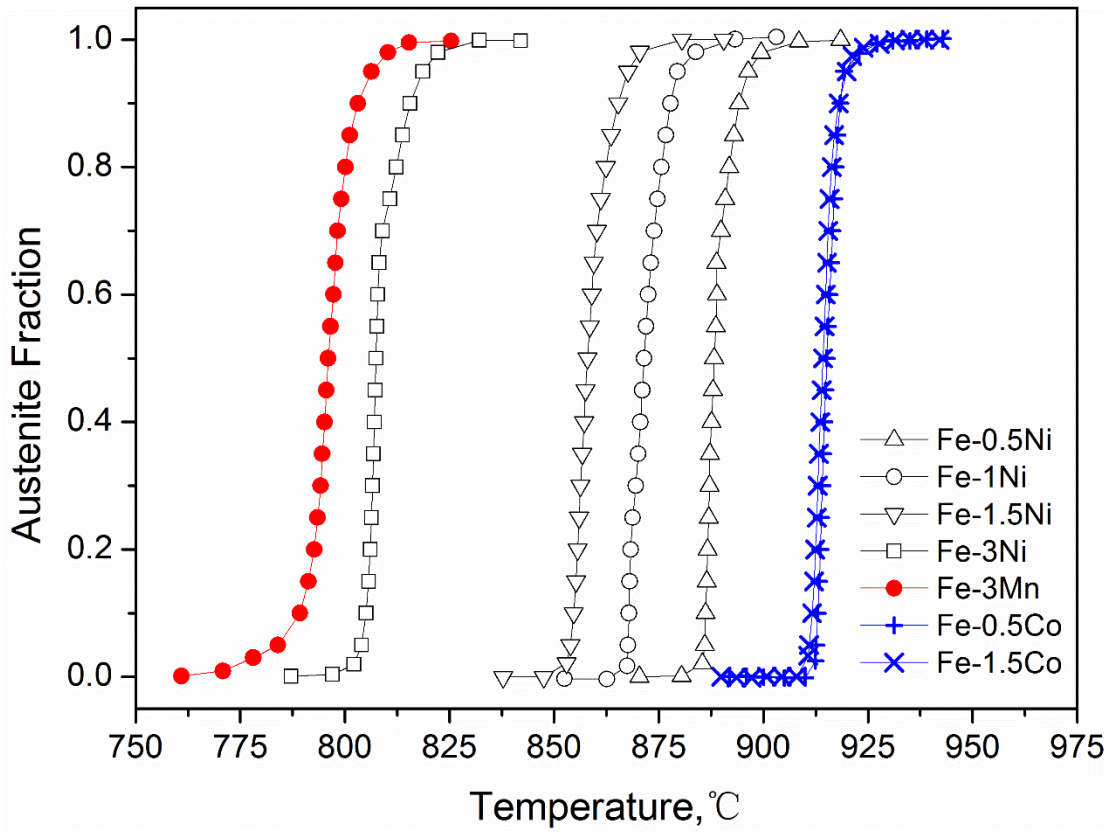

Fig. 5 Overall kinetics of the ferrite to austenite transformation upon heating at a rate of 1 K/s in the Fe-Ni, Fe-Mn and Fe-Co alloys.

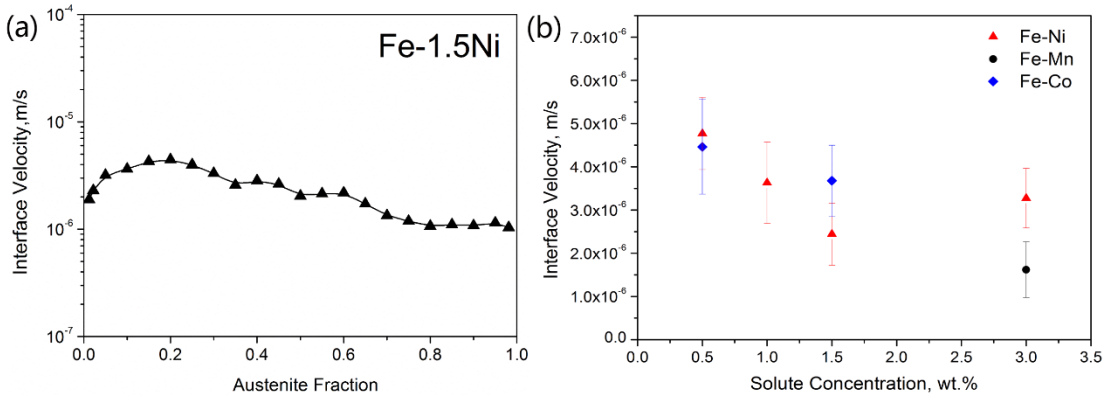

Fig. 6 (a) The interface velocity as a function of austenite fraction in the Fe-1.5Ni alloy. (b) The average interface velocities during the ferrite to austenite transformation as a function of solute concentration.

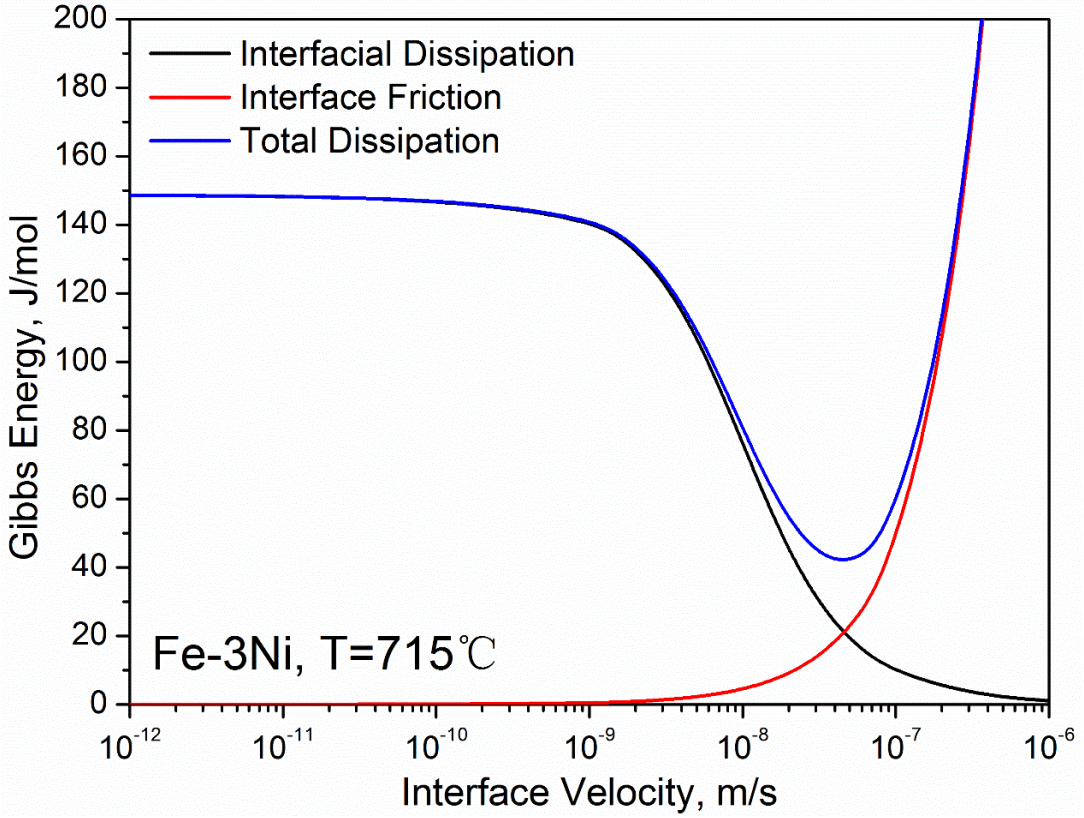

Fig. 7 The energy dissipation at the migrating interface as a function of interface velocity during the austenite to ferrite transformation in the Fe-3Ni alloy at 715 ℃.

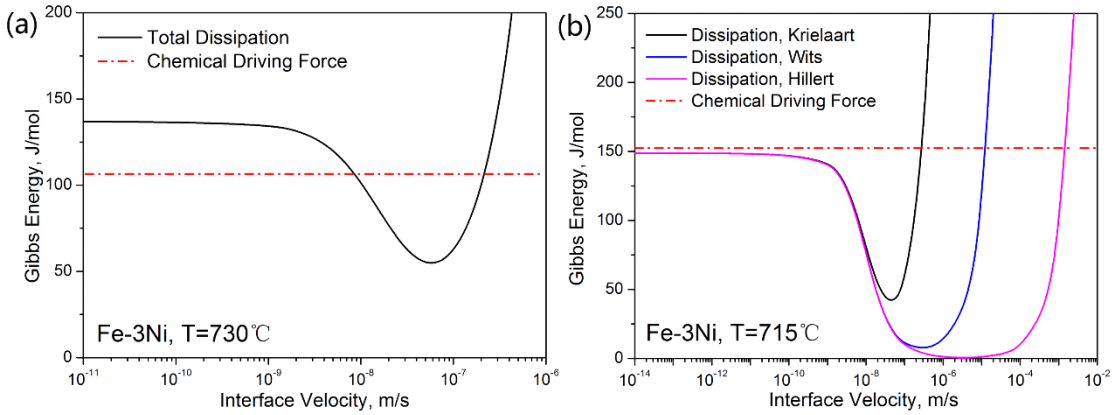

Fig. 8 Total Gibbs energy dissipation and the available chemical driving force as a function of interface velocity for the γ→α transformation in an Fe-3Ni alloy (a) at 730 ℃and (b) at 715 ℃.

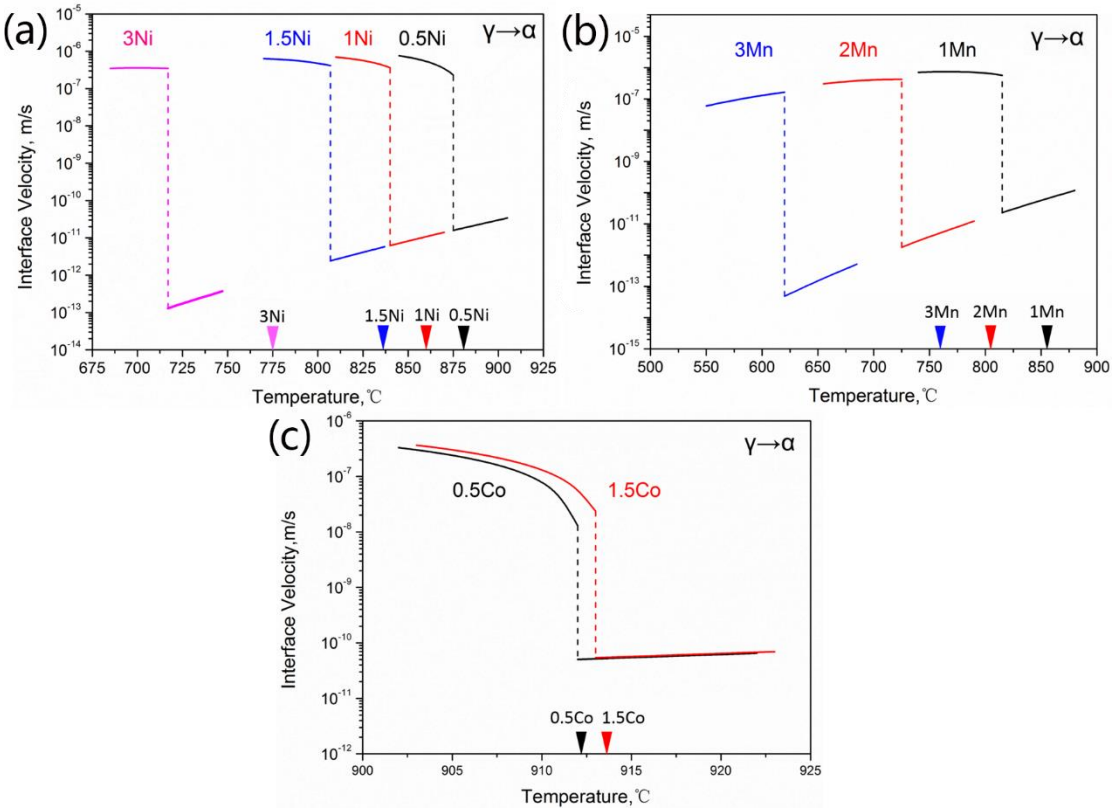

Fig. 9 The predicted interface velocities as a function of temperature for the γ→α transformation in (a) Fe-Ni (b) Fe-Mn and (c) Fe-Co alloys. The corresponding T_0 temperatures are labelled with the solid arrows

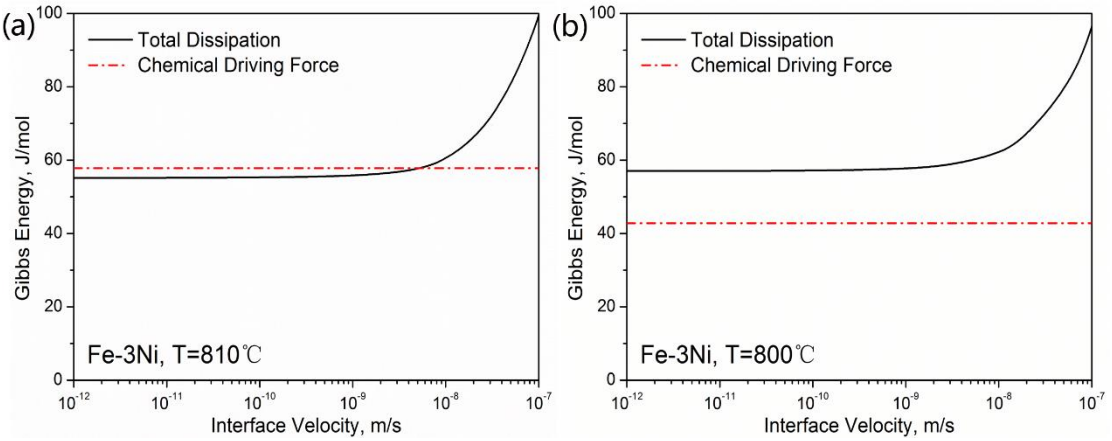

Fig. 10 Total Gibbs energy dissipation and the available chemical driving force as a function of interface velocity for the α→γ transformation in Fe-3Ni (a) at 800 ℃and (b) at 810 ℃.

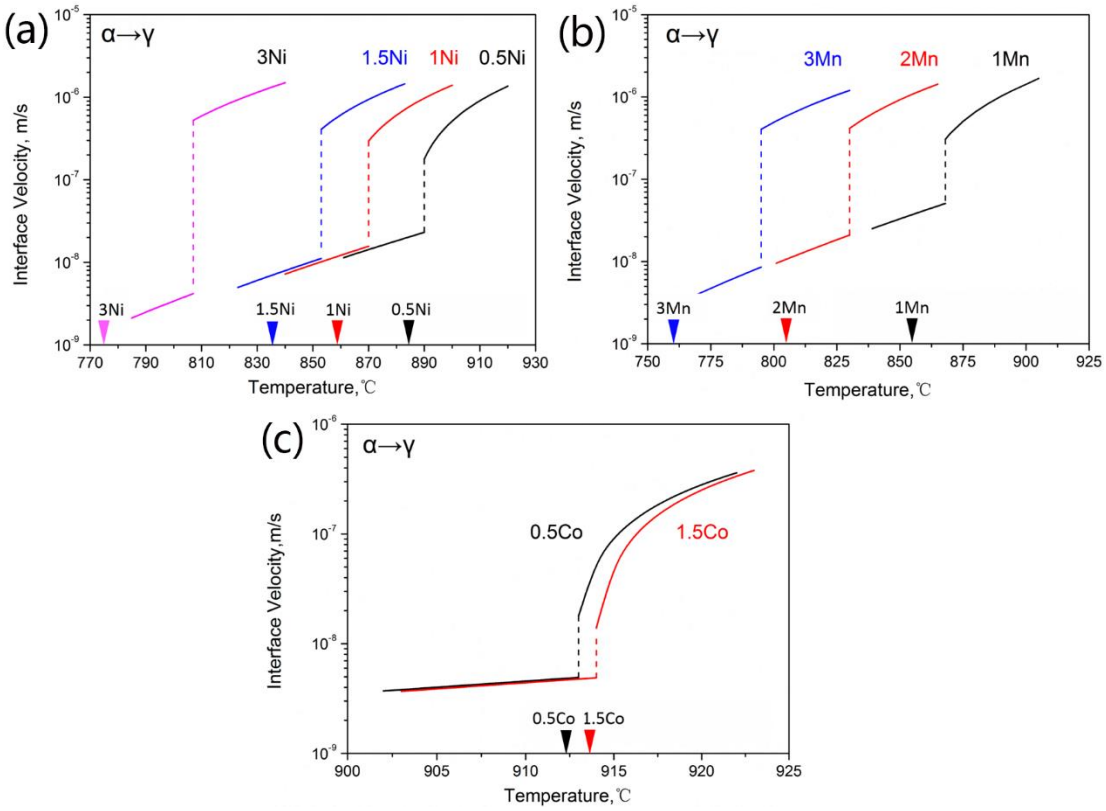

Fig. 11 The predicted interface velocities as a function of temperature for the α→γ transformation in (a) Fe-Ni (b) Fe-Mn and (c) Fe-Co alloys with different solute concentration. The corresponding T_0 temperatures are labelled with the solid arrows

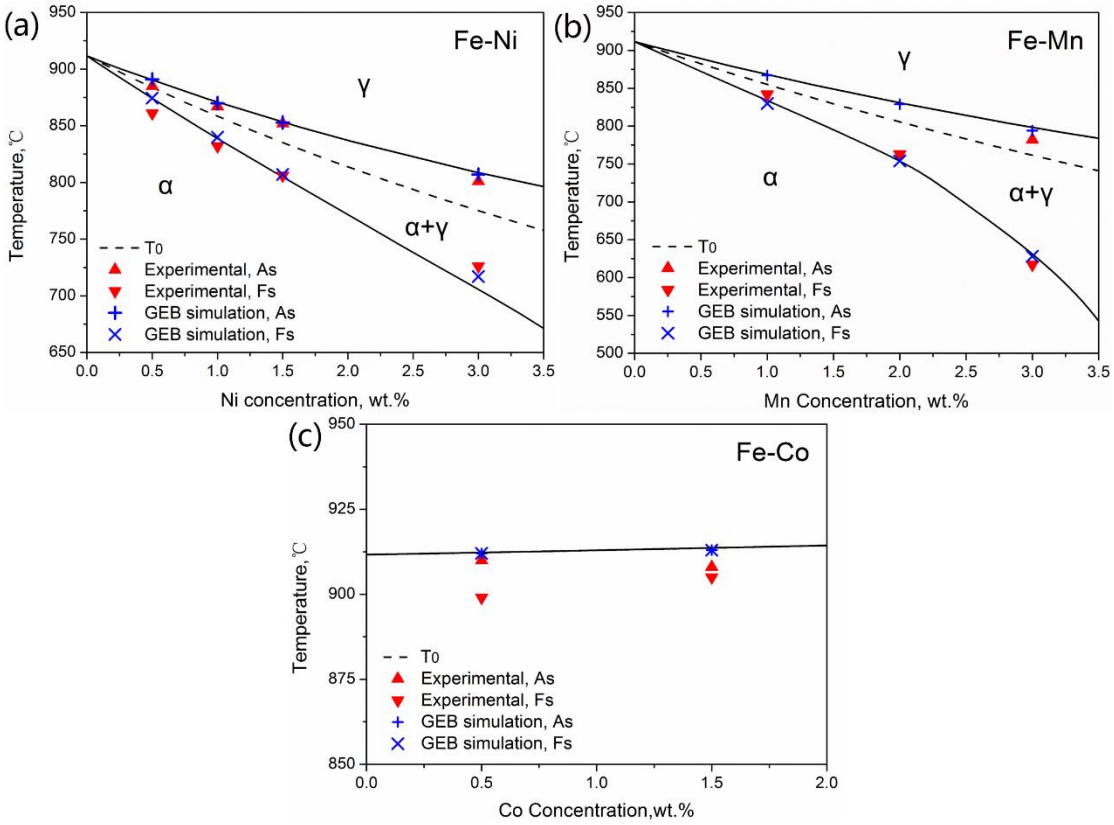

Fig. 12 Comparison between model predictions and experimental measurements of the onset temperatures for the austenite to ferrite transformation and ferrite to austenite transformations in the (a) Fe-Ni (b) Fe-Mn and (c) Fe-Co alloys.

Note: (1) Experimental data of the Fe-1Mn and Fe-2Mn alloys are obtained from [9].

(2) The A_{e1}, A_{e3} and T_0 lines overlap in the Fe-Co diagram so that only one solid line is visible.

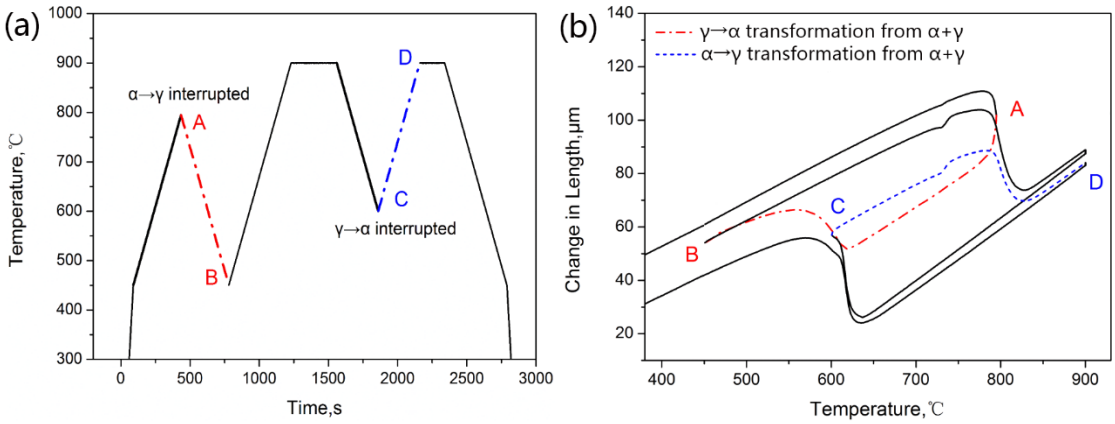

Fig.13 (a) Sketch of heat treatment (b) Dilatation curve of the specimen as a function of temperature.

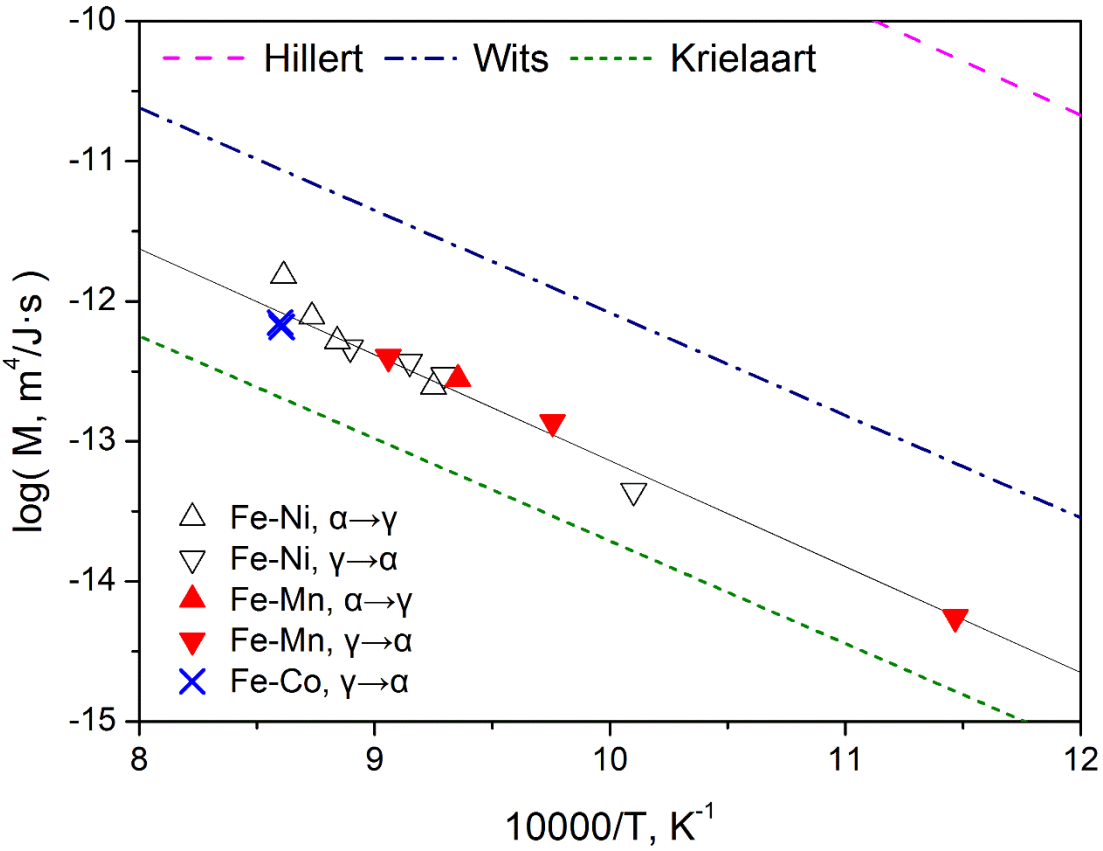

Fig.14 The derived intrinsic interface mobility as a function of temperature.